*J Mater Sci* (2021) 56:14518–14530

Chemical routes to materials

# Effects of pre-imidization on rheological behaviors of polyamic acid solution and thermal mechanical properties of polyimide film: an experiment and molecular dynamics simulation

Daolei Lin[1], Runyue Li[1], Tengfei Li[1], Yucheng Zi[1], Shengli Qi[1,2,*], and Dezhen Wu[1,2,*]

[1] State Key Laboratory of Chemical Resource Engineering, Beijing University of Chemical Technology, Beijing 100029, China
[2] Changzhou Institute of Advanced Materials, Beijing University of Chemical Technology, Changzhou 213164, Jiangsu, China

**Received:** 3 March 2021
**Accepted:** 6 June 2021
**Published online:** 16 June 2021



## ABSTRACT

A series of polyamic acid (PAA) solutions and corresponding polyimide (PI) films with different chemical structures were prepared through a partial pre-imidization process, and the rheological behavior of PAA solutions and thermal mechanical properties of PI films were investigated in detail. The FT-IR spectra indicate that the pre-imidization degree (pre-ID) of PI could be accurately controlled by adjusting the amount of dehydration reagents. The PI films with a certain pre-ID exhibit better mechanical properties and lower coefficient of thermal expansion. The viscosity curves of PAA solution with varying shear rate show that the PAA solutions with high pre-ID have low shear sensitivity, which exhibits a lower viscosity at the low shear rate, but retains almost the same viscosity at high shear rate. Chain conformation variations with pre-IDs and solvent content were investigated by molecular dynamic (MD) simulation. The MD results indicate that a sudden increase in cohesive energy density leads to gel at a certain pre-ID and the mobility of molecular chain decreases greatly with solvent volatilization. It is supposed that the molecular chain orientation induced by the pre-imidization will be preserved in the subsequent thermal imidization process. Therefore, the PI films with a certain pre-IDs exhibit more excellent thermal mechanical properties, especially for the PI with rigid-rod segments.

Handling Editor: Yaroslava Yingling.

Address correspondence to E-mail: qisl@mail.buct.edu.cn; wdz@mail.buct.edu.cn



https://doi.org/10.1007/s10853-021-06241-1

## Introduction

Polyimide (PI) has drawn tremendous attention in the application areas of microelectronics, engineering, and aerospace industries for their outstanding thermomechanical properties, excellent dimensional stability, good dielectric properties and high resistance to chemical and solvent [1–4]. The soluble and thermoplastic PIs can be obtained via polycondensation and cyclodehydration reactions at a temperature 140–180 °C without isolation of the precursor in solution [5]. However, most of PIs are prepared from the conventional two-step method due to their insoluble and infusible characteristics, which includes the synthesis of polyamic acid (PAA) and subsequent thermal treatment [6]. Despite the development of high-performance PI films has made significant progresses in the past decades, the properties of PI films still require urgent improvement when employed in extreme circumstances.

Many previous researchers expected to obtain PI films with better performance by changing the structures of PI or incorporating multiple components. Effects of monomer structure and imidization degree on thermoplastic PI films were investigated by Saeed et al. [7], the results showed that a change in viscoelastic behavior from liquid-like to solid-like with increasing the imidization degree. Zhou et al. [8] prepared a series of crosslink PI films with ultralow coefficient of thermal expansion (CTE) using 1,3,5-tris(4-aminophenoxy)benzene (TAPOB) as the crosslinker, which broke the mutual restraints between low permittivity and low CTE in PI films. Li et al. [9] found that the introduction of trifluoromethyl (-$CF_3$) groups could substantially reduce the dielectric permittivity of PI films, which was attributed to the branched and bulky structure in -$CF_3$ groups restrain chain packing effectively by reducing intermolecular force significantly [10, 11]. Tong et al. [12] prepared the fluorinated PI films derived from 6FDA and novel aromatic diamines with pendent phenyl structure, the high fractional free volume endowed these films with excellent solubility, high permeability coefficients and outstanding mechanical properties. It has been found that the introduction of rigid-rod segments could enhance the degree of crystallinity and mechanical properties of PI simultaneously [13–15]. However, when the ether linkage or carbonyl group which could improve the mobility of molecular chains was introduced to the backbone, the flexible groups in PI chains increased the order degree and decreased the mechanical properties [16–18]. New poly(imide-benzoxazole) copolymers containing benzoxazole moieties were fabricated [19, 20], and the excellent thermal stability, mechanical performance, environmental resistance and hydrolytic stability of these copolymers enable them to be used in electrical and electronic applications. Musto et al. [21] studied the curing behavior, morphology and mechanical properties of PI/silica nanocomposites, and the results demonstrated that the nanocomposites exhibited better mechanical properties even at a high temperature of 250 °C. Gao et al. [22] obtained a series of novel nano-ZnO/hyperbranched PI hybrid films by the in situ sol–gel polymerization method, and the hybrid films exhibited unique photophysical processes for fluorescence compared with the physical blend of ZnO nanoparticles and PI matrix. Chiang et al. [23] investigated the physical and mechanical properties of PI/titania hybrid films, and the results indicated that the incorporation of small amount of titania endowed hybrid films lower thermal expansion and resistivity. Chen et al. [24] fabricated high mechanical properties PI nanocomposite films containing functionalized graphene sheets via in situ thermal preparation.

Recently, considering the high commercial cost of novel diamines and dianhydride monomers, researchers start to pay more and more attentions to the effect of imidization process on improving the performance of PI materials. Lin et al. [25] studied the structural evolution of PI macromolecular chain during pre-imidization process by molecular dynamic (MD) simulation. The results suggested that the aggregation structure tended to looser chain packing and more extended chain conformation during the pre-imidization process. The effects of chemical structure and pre-imidization on the aggregation structure and properties of PI films were investigated [26–28], and the PI films derived from solution of higher pre-imidization exhibited more ordered aggregation structure and better mechanical properties. The PI films with a certain degree of pre-imidization owned a relatively low CTE [29, 30], which was mainly due to that the chemical pre-imidization promoted the in-plane orientation of molecular chains. Near-surface structure formation in chemically imidized PI films was measured with a nanoindentation setup, and crosslinking reactions in

PIs at temperatures over 400 °C were suggested to account for the higher modulus of the air side of the samples annealed at 400 °C than the casting side [31]. A series of PI fibers were also prepared through a partial pre-imidization process [32, 33], and it was observed that the partial rigid-rod and oriented PI chains in the chemical pre-imidization process led to the effective enhancement in the mechanical properties of PI fibers. The MD simulations of the imidization of adsorbed PAA demonstrated that local chain motion instead of large-scale chain rearrangement is necessary for the imidization of interfacial chains [34]. The residual stress of PI films with different imidization processes was also studied, and the amount of residual solvent and pre-baking time during imidization process brought the difference in the residual stress [35, 36]. Su et al. [37] synthesized a series of ternary copolyimide fibers via partly imidization method, and the results indicated that the partly imidized PAA owned higher intrinsic viscosity than that of pure PAA, the as-spun fibers exhibited a circular and dense internal morphology. Park [38] obtained a high draw ratio of the as-spun PAA fiber by adding acetic anhydride and pyridine to the PAA solution to make it slightly gelled. It was found that the diffusion rate of dimethylacetamide became slower and the solution viscosity increased because of the conversion of PAA to the corresponding PI. Besides, various new characterization techniques have been utilized to investigate the evolution of these structures and properties in the imidization process [39, 40].

In the present work, a series of PAA solutions and corresponding PI films derived from pyromellitic dianhydride (PMDA)/4,4′-oxydianiline (ODA), 3,3′,4,4′-biphenyldianhydride (BPDA)/ODA and BPDA/p-phenylene diamine (PDA) were obtained via a partial pre-imidization process. The effect of the amount of dehydration reagents on the pre-IDs was measured by FT-IR spectroscopy. Rheological behavior of PAA solutions was characterized and used to evaluate the processability of PI films in the coating process. Mechanical properties and CTE were also measured in order to study the effects of pre-IDs on the thermal mechanical properties of PI films. Besides, the corresponding composite models with different pre-IDs and solvent content were constructed and analyzed based on MD simulation, and the cohesive energy density (CED) and interaction energy in the composite models were calculated. The mobility of PAA chain varied with the solvent content was predicted by mean square displacement (MSD). In a word, this work clarified the effect of chemical pre-imidization on the rheological behavior of PAA solutions and thermal mechanical properties of PI films at molecular dynamic level.

## Experiment section

### Materials

The monomers PMDA and BPDA were purchased from Shi Jiazhuang Hai Li Chemical Company and purified by sublimation prior to use. The monomers PDA and ODA were supplied by Jinan Shi Ji Tong Da Chemical Company and recrystallized in ethyl acetate prior to use. The solvent dimethylacetamide (DMAc), acetic anhydride and pyridine were purchased from Tianjin Fu Chen Chemicals Reagent Factory.

### Preparation of PAA solutions and PI films

The PAA solutions derived from PMDA/ODA, BPDA/ODA and BPDA/PDA were synthesized, firstly. Take the polymerization of PMDA/ODA PAA solution as an example, the diamine ODA was dispersed firstly in DMAc solvent with stirring at room temperature. An equimolar amount of PMDA was added in several portions to the solution after the diamine was almost dissolved. After stirring at a low temperature (-5—0 °C) for 5 h, a yellow viscous PAA solution with 15 wt% solid content was obtained. The PAA solution was divided equally into six portions, and then, different mole amounts of dehydration reagents (molar ratio of pyridine/acetic anhydride = 2/1) were added into the PAA solutions. The mixtures were stirred for 5 h at room temperature to yield homogeneous PAA-PI solutions with theoretical pre-ID of 0%, 10%, 20%, 30%, 40% and 50%. Then, the prepared solutions were cast onto dust-free glass plates using an adjustable doctor blade followed by thermal treatment in a temperature-programmable oven for 24 h at 60 °C to obtain the PAA-PI films, and the fully imidized PI films were obtained by heating the PAA-PI films for 1 h at 135 °C and then 2 h at 300 °C.

The synthesized PI − PAA (PI) films and solutions with theoretical pre-IDs of 0%, 10%, 20%, 30%, 40% and 50% were abbreviated as PAA-PI (PI) 0, PAA-PI (PI) 10, PAA-PI (PI) 20, PAA-PI (PI) 30, PAA-PI (PI) 40 and PAA-PI (PI) 50, respectively.

## Characterization

FT-IR spectroscopy was recorded on a Nexus 670 spectrometer with the scanning wavenumbers ranging from 4000 to 400 $cm^{-1}$. The band at 1377 $cm^{-1}$ (C − N stretching of the imide ring) was selected for quantifying the pre-ID, and the aromatic band at 1496 $cm^{-1}$ (C − C stretching of the p-substituted benzene backbone) was selected as the internal standard. The corresponding pre-IDs were calculated using the following equation:

$$pre-ID(\%) = \frac{(S_{1377}/S_{1496})_{T=60}}{(S_{1377}/S_{1496})_{T=300}} \times 100\% \quad (1)$$

Here, S is the area of the absorption band; T = 60 °C is the treatment temperature of films, and T = 300 °C is taken as the temperature of complete cyclodehydration.

The rheological characterization for all samples was conducted on the hybrid rheometer DISCOVERY HR-1, equipped with a 25 mm diameter parallel plate fixture and a gap setting of 1 mm for all the measurements. The steady shear sweep and dynamic frequency sweep measurements were performed within the shear rate range between 0.1 and 100 $s^{-1}$ and oscillation frequency range from 0.5 to 500 rad/s, respectively. The experimental temperature was set at 35 °C. After loading the PAA solution, a thin layer of silicone oil was applied to cover the exposed edge in order to preventing the solvent evaporation.

An ultraviolet (UV) transmittance spectrum was produced on a UV − vis spectrophotometer (UV-2500) manufactured by SHIMADZU, Japan. The transmittance mode was adopted, and the spectral range was 200–800 nm.

The dynamic thermomechanical analysis (DMA) was carried out on a DMA Q800 system with a load frequency of 1 Hz at a heating rate of 5 °C/min from 50 to 450 °C.

Thermal mechanical analysis (TMA) was determined using a TMA Q400 analyzer to measure the coefficient of thermal expansion (CTE) of the PI films at a preload force of 0.05 N and a heating rate of 5 °C/min from 50 to 200 °C in nitrogen.

Thermogravimetric analysis (TGA) was performed with a TGA Q50 instrument at a heating rate of 10 °C/min from 50 to 800 °C. The samples weighing about 5.0 mg were tested in air.

Mechanical properties of PI films were performed at room temperature on a SANS CMT 4001 tensile apparatus with dumbbell-shaped specimens with the crosshead speed of 10 mm/min.

## Molecular simulation details

The amorphous cell construction establishment and simulation in this work were performed using Materials Studio 8.0, and 10 PI chains with 20 repeat units [41–43]. The MD simulation of PI composite models with different pre-IDs and solvent content was designed in accordance with the experimental PAA-PI solutions and was packed into a periodic box for the amorphous cell construction. The initial density of the amorphous cells was set to 0.1 $g/cm^3$, and the Forcite module was used to optimize the molecular structure with COMPASS as the force field. The Nose thermostat and Berendsen barostat were used to control the temperature and pressure in the amorphous cell equilibrium process. NPT ensemble and NVT ensemble were employed to obtain the final equilibrium model [25, 44–47]. 300 ps MD in the NPT ensemble at 0.5 GPa and 298 K was carried out to compress the cell to experimental density. NVT annealing dynamics was then performed at 598 and 298 K, each about 300 ps. Relax the cell by a subsequent 300 ps MD in the NPT ensemble at 0.0001 GPa and 298 K to check the course of density fluctuations until the density-time curve was stable. Finally, 1000 ps MD was performed in NVT ensemble at 0.0001 GPa and 298 K in order to further improve the equilibration. CED, interaction energy and MSD curves of composite models with different pre-IDs and solvent content were estimated by Forcite analysis tools.

## Results and discussion

### PAA with different pre-IDs prepared via chemical imidization

The FT-IR spectra of PAA-PI films with different chemical structures and different amounts of dehydration reagents are presented in Fig. 1. It can be seen that the characteristic peaks of PI at 1777, 1717, 1377 and 724 $cm^{-1}$ (1777 and 1717 $cm^{-1}$ for C = O asymmetrical and symmetrical stretching, respectively,1377 $cm^{-1}$ for C-N stretching and 724 $cm^{-1}$ for C = O bending of imide ring) increased obviously with increasing dehydration reagents, suggesting that the successful formation of the imide group. Moreover, the characteristic absorption band of isoimide groups at 1800 $cm^{-1}$ is not detected in the spectra, indicating that the effects of isoimide can be ignored. The pre-IDs of experimental films based on Eq. (1) were calculated and summarized in Table 1. Apparently, the experimental data approached to the theoretical ones, indicating that the pre-IDs of PI could be accurately controlled by adjusting the amount of dehydration reagents. It is found that when the theoretical pre-IDs of PMDA/ODA, BPDA/ODA and BPDA/PDA PAA solutions exceeded 30%, 40% and 20%, respectively, gel occurred, resulting in the inability to obtain the corresponding PI films. Besides, the intrinsic viscosities of the PAA-PI solutions are reduced slightly with increasing the pre-IDs. The PI films obtained by heating the PAA-PI films with different pre-IDs exhibited the same absorption bands, as shown in Fig. 1, indicating that the final PI films get fully imidized.

UV transmission spectra of PI-PAA solutions with different pre-IDs are recorded in Fig. 2. The wavelength with a transmittance of 1% is defined as the cut-off wavelength. It can be seen that the cut-off wavelength of PAA-PI solutions with different chemical structures obviously increased with increasing pre-IDs, which can be attributed to the conjugation effect of imide and benzene rings that promoted the movement of electrons. The color of the PAA-PI solution varied with the pre-IDs in a digital photograph, as shown in Fig. 2, which more intuitively illustrated the enhanced conjugation effect with pre-IDs, accounting for the darkened colors.

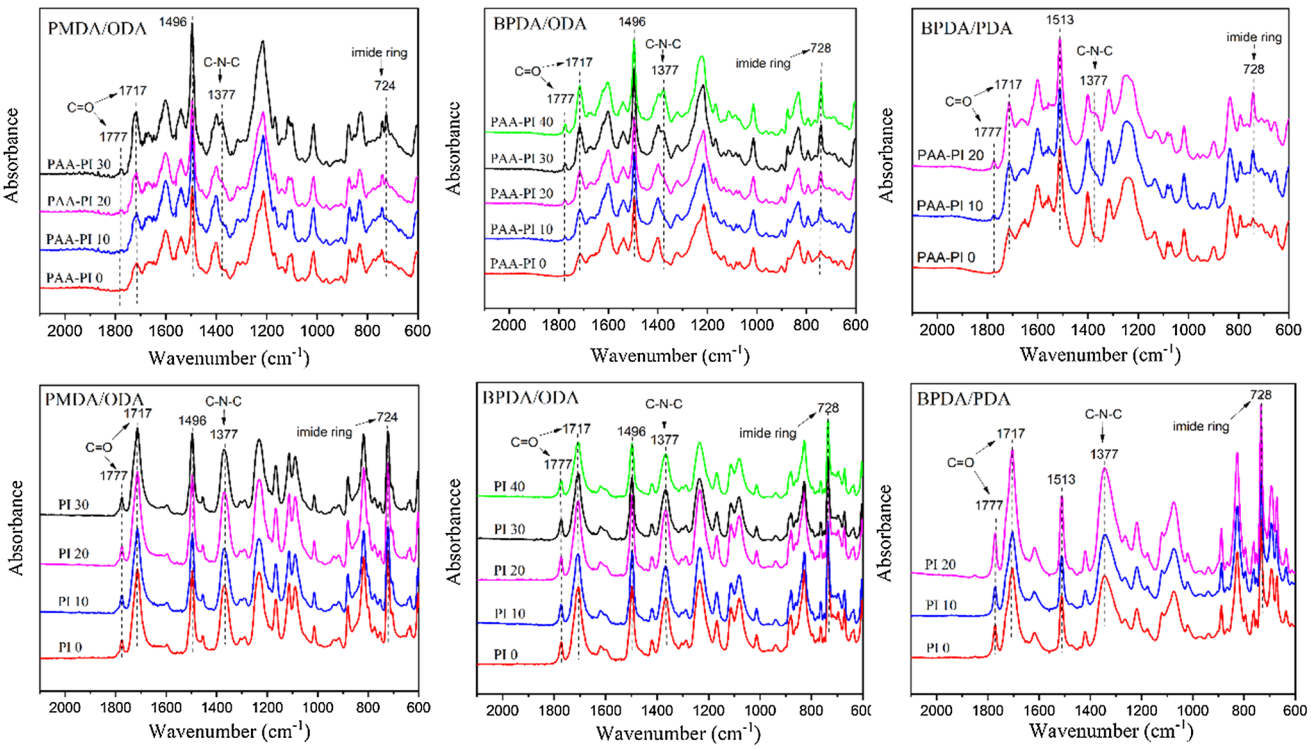


**Figure 1** FT-IR spectra of the PAA-PI and PI films with different amounts of dehydration reagents.

**Table 1** Experimental pre-IDs of PAA-PI films and intrinsic viscosity of PAA-PI solutions with different chemical structures and different amounts of dehydration reagents

| Theoretical pre-IDs (%) | PMDA/ODA | | BPDA/ODA | | BPDA/PDA | |
|---|---|---|---|---|---|---|
| | Experimental pre-IDs (%) | Intrinsic viscosity (dL/g) | Experimental pre-IDs (%) | Intrinsic viscosity (dL/g) | Experimental pre-IDs (%) | Intrinsic viscosity (dL/g) |
| 0 | 0 | 1.59 | 0 | 1.94 | 0 | 1.77 |
| 10 | 9.8 | 1.53 | 9.6 | 1.88 | 9.7 | 1.74 |
| 20 | 19.3 | 1.52 | 19.8 | 1.86 | 19.6 | 1.73 |
| 30 | 28.9 | 1.47 | 29.3 | 1.86 | gel | / |
| 40 | gel | / | 38.8 | 1.85 | gel | / |
| 50 | gel | / | gel | / | gel | / |

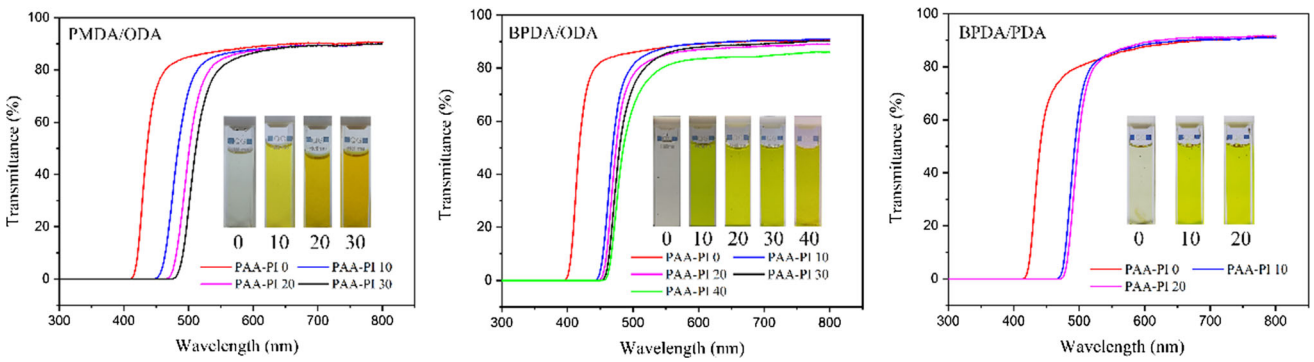


**Figure 2** Transmittance of PAA-PI solutions with different pre-IDs.

## Rheological behavior of PAA solutions with different pre-IDs

Rheological properties have an important influence on the processing of PI films. The apparent viscosities of PMDA/ODA, BPDA/ODA and BPDA/PDA PAA solutions with different pre-IDs in the steady shear measurements are compared in Fig. 3. The PAA solutions exhibit remarkable shear-thinning behaviors, indicating a typical non-Newtonian liquid. The results are attributed to the high shear rate induced the ordered arrangement of PAA-PI chains, and a coil-to-stretch transition occurred as the molecular chains experienced the maximum shear rate. The viscoelastic properties of entangled polymers are understood in terms of the reputation concept, i.e., the orientation of PAA-PI chains is the extension of pipe, which decreased the crawling resistance so as to decrease the viscosity [48]. Meanwhile, the PAA-PI solutions with high pre-IDs exhibited a lower viscosity at the same shear rate. This is attributed to pyridine/acetic anhydride which acts as both dehydration reagent and diluent for PAA solutions. Besides, the rigidity of PI segment is greater than that of PAA due to the presence of imide ring, leading to the viscosity of PAA-PI solutions decreased with increasing pre-IDs at the same shear rate. Moreover, we can find that the shear-thinning phenomenon of the PAA-PI solutions with lower pre-IDs is more obvious. The viscosity curves of PAA-PI solutions with different pre-IDs intersect at one point at high shear rates, suggesting that the viscosity decrease in PAA-PI solution caused by the increased pre-IDs has no influence on the PI film processing process at high shear rate.

The logarithmic plots of storage modulus (G′) and loss modules (G″) are also shown in Fig. 3 as a function of angular frequency. Both G′ and G″ obviously decreased with the pre-IDs of PAA-PI solutions. This could be attributed to the fact that the viscoelastic behavior of polymer solutions is related to chain entanglement, and the PAA-PI molecule chains gradually became extended from entanglement with increasing the pre-IDs. The G″ is higher

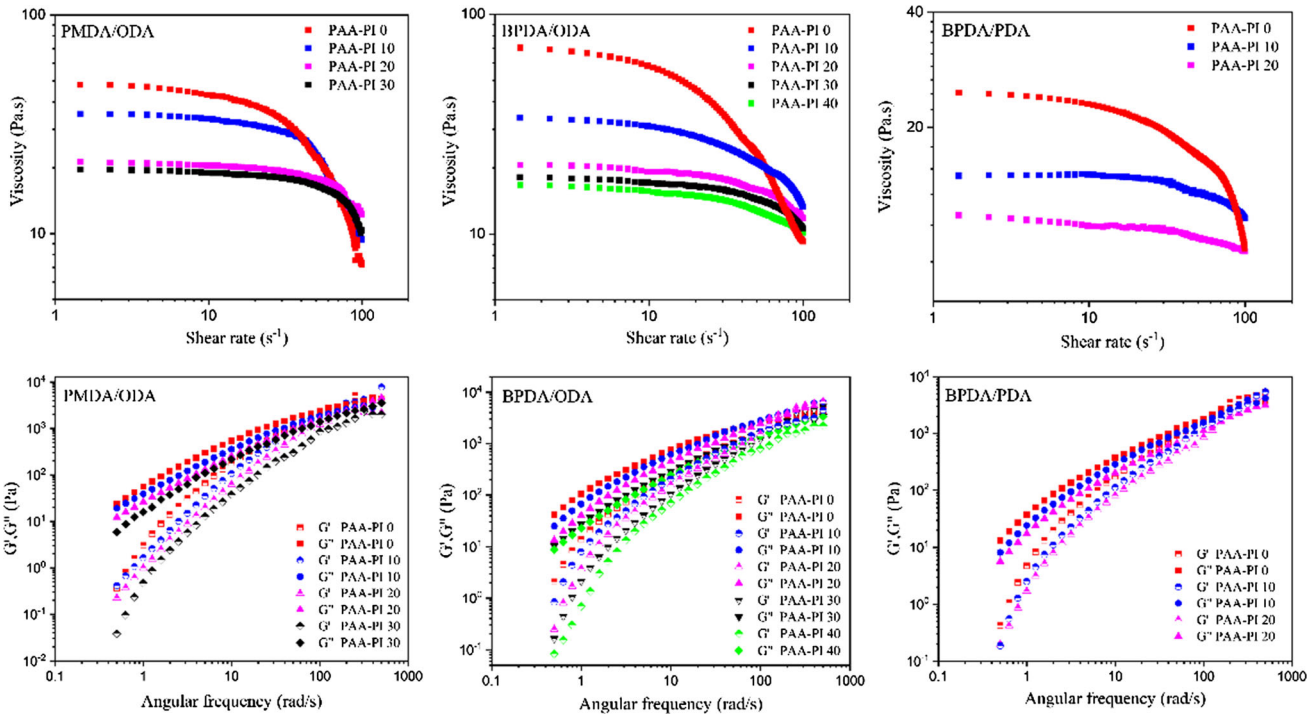


**Figure 3** Viscosity as a function of shear rate and angular frequency dependence of storage modules (G ') and the loss modules (G") for PAA-PI solutions varies with the pre-IDs.

than the G′ at the low angular frequency region, which is a characteristics behavior for viscoelastic fluids [49]. In a word, both G′ and G" increased with increasing angular frequency, and the plateau modulus appeared at high angular frequency region indicated a typical solid-like behavior [50]. It is probably due to the hydrodynamic drag force exerted by the solvents at high angular frequency, which stretched the PAA-PI chains from its equilibrium coiled to stretched states [51].

## Thermal and mechanical properties of PI films

The mechanical properties of final PI films based different pre-IDs are presented in Fig. 4, the results concluded that the tensile strength and modulus of final PI films increased with increasing the pre-IDs. It's worth noting that the mechanical properties of the BPDA/PDA film increased most at the same pre-ID of 20%, followed by the PMDA/ODA film, and the mechanical properties of the BPDA/ODA did not increase significantly with increasing the pre-IDs. The same regularity was also found for the CTE of final PI films varies with different pre-IDs, as shown in Fig. 5.

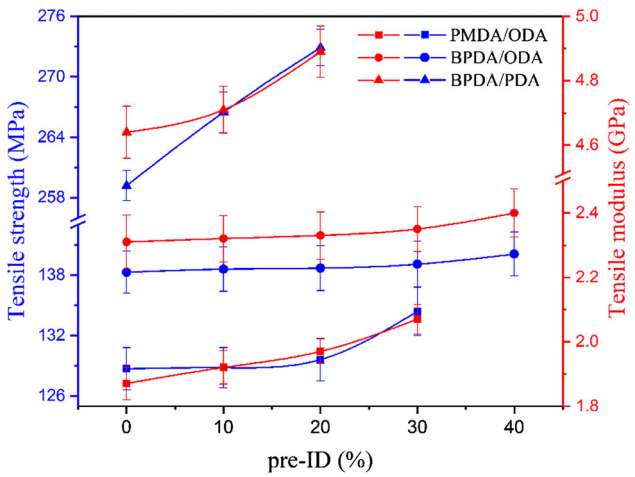


**Figure 4** Tensile strength and modulus of PI films with different pre-IDs.

The CTE of BPDA/PDA film with pre-ID of 20% was reduced by 34.7% compared with the single thermal imidization film. However, the CTE of BPDA/ODA film decreased only 4.9% when the pre-ID reached 40%. As mentioned above, it can be seen that the PI with a higher rigidity is influenced more significantly by the chemical pre-imidization process. We speculated that the reason for this phenomenon is that the C–O–C bond in the ODA made the PMDA/ODA-

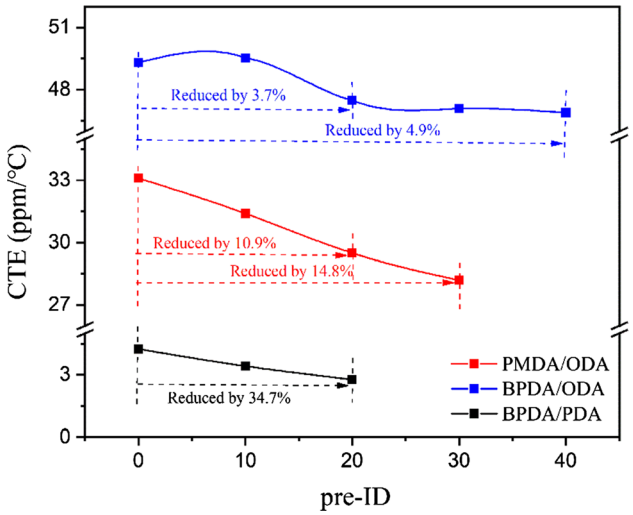


**Figure 5** CTE of PI films with different pre-IDs.

and BPDA/ODA-based PAA-PI molecular chain at a certain pre-ID still in a random entanglement state.

The thermal stabilities of the PI films with different pre-IDs were evaluated by TGA measurements in an air atmosphere as collected in Fig. 6, and we can find that the PMDA/ODA-, BPDA/ODA- and BPDA/PDA-based PI films exhibited 5% weight loss temperature at 538.8 °C, 549.6 °C and 582.1 °C, respectively, which are independent of the pre-IDs. This is attributed to the thermal decomposition of PI mainly related to the chemical structure, and FT-IR spectra presented in Fig. 1 have indicated the same chemical structures of the final PI films. The $T_g$ of PI fibers increased slightly with a substantial increase in draw ratio, because of the molecular orientation restricted the molecular chain mobility [52]. The PI films with a certain pre-IDs have a relatively lower plane orientation compared with the fibers with a large draw ratio. Therefore, the $T_g$ of PI films with different pre-IDs is almost the same, as presented in Fig. 7. The $T_g$ of the PMDA/ODA-, BPDA/ODA- and BPDA/PDA-based PI films is 389.8 °C, 292.7 °C and 354.4 °C, respectively.

## Chain mobility and conformation variation of PAA with different pre-IDs in solvent

To our knowledge, the conformation evolution of PAA-PI chain in solvent during the pre-imidization process is still unclear due to the lack of effective characterization methods. To get a deep insight into the pre-imidization, structure and properties relationship of PI, the mobility of PAA-PI chains and their interaction energy with the solvent molecules in the pre-imidization were calculated by MD simulation. The CED is a parameter which depends on breaking all intermolecular interactions in a unit volume. Wholly speaking, the CED of PAA-PI solutions showed a downward trend with the continuous increase in pre-IDs, as shown in Fig. 8. However, the CED of PMDA/ODA, BPDA/ODA and BPDA/PDA solutions all exhibits a turning point at the pre-IDs of 40%, 60% and 20%, respectively, which indicated that the intermolecular interactions in a unit volume increased suddenly at those pre-IDs. Specifically, the pre-IDs at the turning point of CED correspond roughly to the pre-IDs when the solution gelled, as listed in Table 1, implying that the gel is attributed to a sudden increase in CED when the pre-IDs increase to a certain value.

The non-bond energy and H-bond energy between PAA-PI chains and solvent molecules with different pre-IDs are listed in Table 2, negative values indicated that non-bond energy and H-bond energy show the attraction between solvent molecules and PI chains. The results showed that the non-bond energy

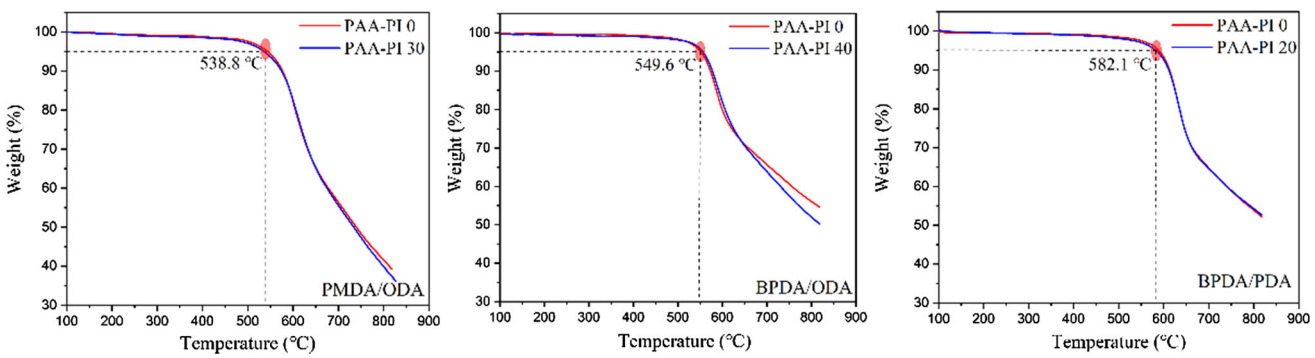


**Figure 6** TGA curves of PI films with different pre-IDs.

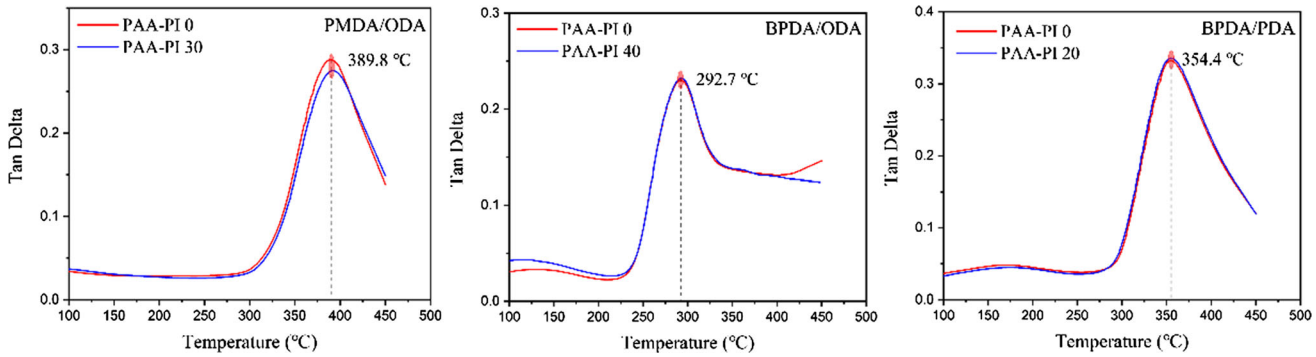


**Figure 7** DMA curves of PI films with different pre-IDs.

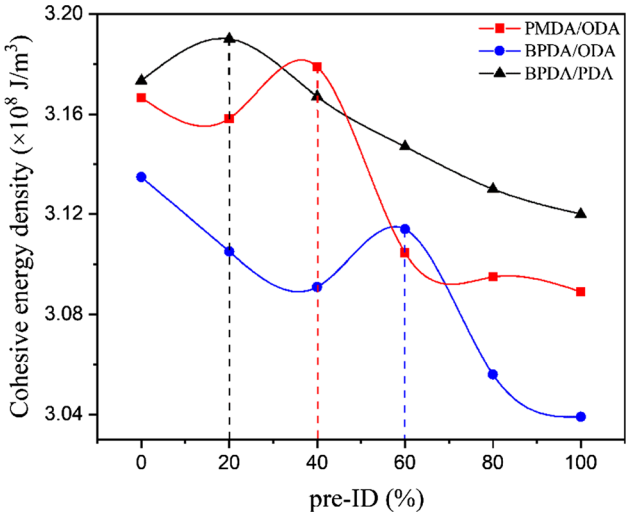


**Figure 8** Cohesive energy density of PAA-PI solutions varies with pre-IDs.

and H-bond energy of the PAA-PI solution composite models decreased with increasing pre-IDs. The decrease in non-bond energy, H-bond energy and CED with the increase in pre-IDs can well explain the viscosity of PAA-PI solutions decreased with increasing dehydration reagents before gel point. After the gel point, the interaction energy between the molecular chains and the solvent molecules continues to decrease, resulting in the phase separation of the polymer and the solvent.

The slope of MSD curves can be used to characterize the mobility of molecular chains in solvent, and the variation of MSD curves of PAA-PI chain with different solvent contents is compared in Fig. 9, taking the pre-ID of 20% for example. We can find that the slope of MSD curves decreased with decreasing the solvent content, illustrating that the volatilization of the solvent limited the mobility of the PAA-PI chains. Our previous study has demonstrated that the PAA-PI chains gradually became extended from entanglement during the pre-imidization process [25]. Schematic diagram illustrating the effect of pre-imidization on molecule structure evolvement is depicted in Fig. 10. The regularity of molecular arrangement formed in pre-imidization process is mostly preserved at the subsequent thermal treatment stage. However, a large amount of solvent has been volatilized before the imidization reaction

**Table 2** Non-bond energy and H-bond energy of PAA-PI solution composite models varies with pre-IDs

| Pre-IDs (%) | PMDA/ODA | | BPDA/ODA | | BPDA/PDA | |
|---|---|---|---|---|---|---|
| | Non-bond energy (kcal/mol) | H-bond energy (kcal/mol) | Non-bond energy (kcal/mol) | H-bond energy (kcal/mol) | Non-bond energy (kcal/mol) | H-bond energy (kcal/mol) |
| 0 | − 44,047 | − 1468 | − 47,758 | − 1577 | − 40,741 | − 1490 |
| 20 | − 42,584 | − 1134 | − 45,491 | − 1201 | − 39,138 | − 1234 |
| 40 | − 40,741 | − 877 | − 43,558 | − 909 | − 37,065 | − 861 |
| 60 | − 37,497 | − 577 | − 41,075 | − 634 | − 34,721 | − 611 |
| 80 | − 36,366 | − 316 | − 38,768 | − 302 | − 32,848 | − 294 |
| 100 | − 34,636 | − 12 | − 36,667 | − 12 | − 30,632 | − 12 |

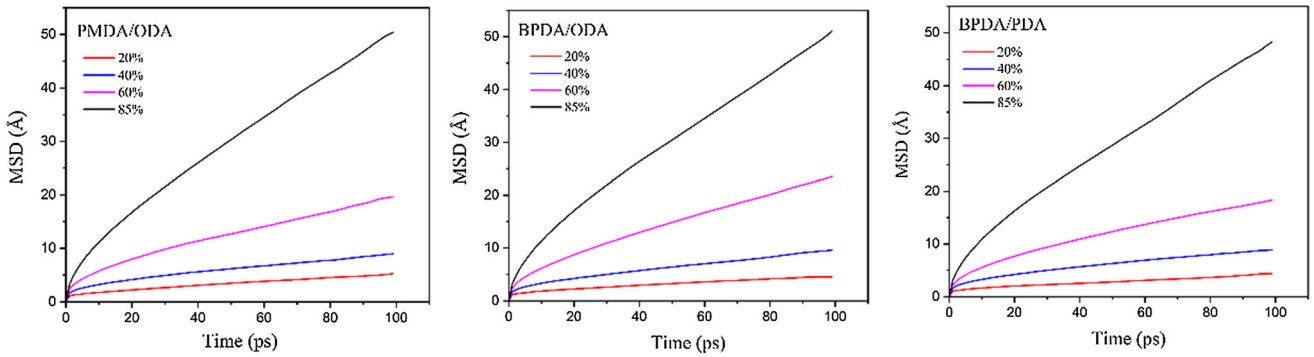


**Figure 9** Mean squared displacement (MSD) curves of PAA-PI models at the pre-ID of 20% with different solvent contents.

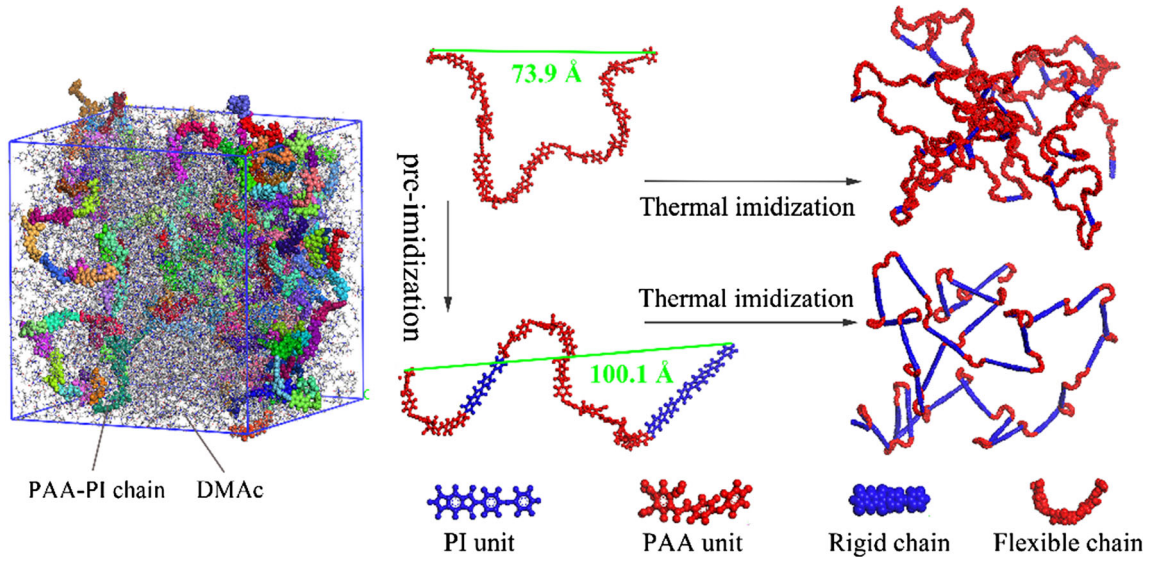


**Figure 10** Schematic diagram illustrating the effect of pre-imidization on molecule structure evolvement.

occurred during the single thermal imidization process, and most of the random coil structure remained in the fully imidized PI films. Therefore, the final PI films possessed a higher plane orientation prepared from PAA-PI solution with a certain pre-ID, as shown in Fig. 10.

## Conclusion

The effects of chemical pre-imidization on the final PI films were investigated by experiment and MD simulation. The pre-IDs of PI films could be accurately controlled by adjusting the amount of dehydration reagents, and the PAA solution with a rigid molecular chain structure gelled at a relatively low pre-ID. Both of the steady and oscillation shear rheological tests indicated that the PAA solutions are a typical non-Newtonian liquid and exhibited remarkable shear-thinning behaviors. Moreover, the PAA-PI solutions with high pre-IDs exhibited a lower viscosity at the low shear rate and almost the same viscosity at high shear rate. The MD simulation result illustrated that the gel of the PAA solution at a certain pre-ID is due to the sudden increase in CED. The MSD curves can well explain that the solvent volatilization in the thermal imidization restricted the mobility of molecular chains. The PI films with a certain pre-IDs exhibited better thermal mechanical properties, especially for the BPDA/PDA PI film with more rigid backbone structure. The CTE of BPDA/PDA film with pre-ID of 20% was reduced by 34.7% compared with the single thermal imidization film, which is attributed to the ordered molecular chains formed in chemical pre-imidization that were preserved in the following thermal imidization.

Therefore, partial chemical pre-imidization has the potential to prepare PI films with more excellent mechanical properties and lower CTE, especially for the PI with rigid-rod segments.

## Acknowledgements

The authors thank the financial support from the National Natural Science Foundation of China [Grant No. 51790501, 51673017, 21404005], the Fundamental Research Funds for the Central Universities (XK1802-2), the National Key Basic Research Program of China [973 program, grant number 2014CB643604, 2014CB643606] and the Natural Science Foundation for Distinguished Young Scholars of Jiangsu Province [Grant No. BK20140006].

## Declarations

**Conflict of interest** The authors declare that they have no conflict of interest.

## References

[1] Okumura H, Takahagi T, Nagai N, Shingubara S (2003) Depth profile analysis of polyimide film treated by potassium hydroxide. J Polym Sci Part B: Polym Phys 41:2071–2078

[2] Song G, Zhang X, Wang D, Zhao X, Zhou H, Chen C, Dang G (2014) Negative in-plane CTE of benzimidazole-based polyimide film and its thermal expansion behavior. Polymer 55:3242–3246

[3] Liaw DJ, Wang KL, Huang YC, Lee KR, Lai JY, Ha CS (2012) Advanced polyimide materials: syntheses, physical properties and applications. Prog Polym Sci 37:907–974

[4] Kreuz JA, Edman JR (1998) Polyimide films. Adv Mater 10:1229–1232

[5] Kuznetov AA, Tsegelskaya AY, Belov MY (1998) Acid-catalyzed reactions in polyimide synthesis. Macromol Symp 128:203–219

[6] Ali AAM, Ahmad Z (2007) The effect of curing conditions and aging on the thermo-mechanical properties of polyimide and polyimide-silica hybrids. J Mater Sci 42:8363–8369 https://doi.org/10.1007/s10853-006-1072-x

[7] Saeed MB, Zhan MS (2006) Effects of monomer structure and imidization degree on mechanical properties and viscoelastic behavior of thermoplastic polyimide films. Eur Polym J 42:1844–1854

[8] Zhou H, Lei HY, Wang JH, Qi SL, Tian GF, Wu DZ (2019) Breaking the mutual restraint between low permittivity and low thermal expansion in polyimide films via a branched crosslink structure. Polymer 162:116–120

[9] Li XL, Lei HY, Guo JC, Wang JH, Qi SL, Tian GF, Wu DZ (2019) Composition design and properties investigation of BPDA/PDA/TFDB co-polyimide films with low dielectric permittivity. J Appl Polym Sci 47989.

[10] Park SJ, Cho KS, Kim SH (2004) A study on dielectric characteristics of fluorinated polyimide thin film. J Colloid Interf Sci 272:384–390

[11] Li J, Zhang G, Zhu Q, Li J, Zhang H, Jing Z (2016) Synthesis and properties of ultralow dielectric constant porous polyimide films containing trifluoromethyl groups. J Appl Polym Sci 134:44494

[12] Tong H, Hu CC, Yang SY, Ma YP, Guo HX, Fan L (2015) Preparation of fluorinated polyimides with bulky structure and their gas separation performance correlated with microstructure. Polymer 69:138–147

[13] Lee C, Iyer NP, Han H (2004) Nanoindentation and optical properties of poly(4,4′-oxydiphenylene p-phenylene pyromellitimide) copolyimide thin films according to the p-phenylene diamine content. J Polym Sci Part B: Polym Phys 42:2202–2214

[14] Kim Y, Ree M, Chang T, Ha CS, Nunes TL, Lin JS (1995) Rodlike/flexible polyimide composite films prepared from soluble poly(amic diethyl ester) precursors: Miscibility, structure, and properties. J Polym Sci Part B: Polym Phys 33:2075–2082

[15] Khatua SC, Maiti S (2002) High performance polymer films 4. Mechanical behavior Eur Polym J 38:537–543

[16] Hsiao BS, Kreuz JA, Cheng SZD (1996) Crystalline Homopolyimides and copolyimides derived from 3,3',4,4'-biphenyltetracarboxylic dianhydride/1,3-bis(4-aminophenoxy)benzene /1,12-dodecanediamine. 2. crystallization, melting, and morphology. Macromolecules 29:135–142

[17] Brandom DK, Wilkes GL (1995) Influence of thermal imidization on the crystallization and melting behaviour of the aromatic polyimide, LaRC CPI-2. Polymer 36:4083–4089

[18] Brillhart MV, Cebe P (1995) Thermal expansion of the crystal lattice of novel thermoplastic polyimides. J Polym Sci Part B: Polym Phys 33:927–936

[19] Hsu SC, Luo GW, Chen HT, Chuang SW (2005) Synthesis and characterization of novel aromatic poly (imide-benzoxazole) copolymers. J Polym Sci Part A: Polym Chem 43:6020–6027

[20] Hsu SC, Chen HT, Tsai SJ (2004) Novel positive-working and aqueous-base-developable photosensitive poly(imide-benzoxazole) precursor. J Polym Sci Part A: Polym Chem 42:5990–5998

[21] Musto P, Ragosta G, Scarinzi G, Mascia L (2004) Polyimide-silica nanocomposites: spectroscopic, morphological and mechanical investigations. Polymer 45:1697–1706

[22] Gao H, Yorifuji D, Wakita J, Jiang ZH, Ando S (2010) In situ preparation of nano ZnO/hyperbranched polyimide hybrid film and their optical properties. Polymer 51:3173–3180

[23] Chiang PC, Whang WT, Tsai MH, Wu SC (2004) Physical and mechanical properties of polyimide/titania hybrid films. Thin Solid Films 447:359–364

[24] Chen D, Zhu H, Liu TX (2010) In situ thermal preparation of polyimide nanocomposite films containing functionalized graphene sheets. Appl Mater Interface 2:3702–3708

[25] Lin DL, Liu YZ, Jia ZQ, Qi SL, Wu DZ (2020) Structural evolution of macromolecular chain during pre-imidization process and its effects on polyimide film properties. J Phys Chem B 124:7969–7978

[26] Wang Y, Yang Y, Jia ZX, Qin JQ, Gu Y (2013) Effect of chemical structure and preparation process on the aggregation structure and properties of polyimide film. J Appl Polym Sci 4581–4587.

[27] Wang Y, Yang Y, Jia ZX, Qin JQ, Gu Y (2012) Effect of pre-imidization on the aggregation structure and properties of polyimide films. Polymer 53:4157–4163

[28] Zhai Y, Yang Q, Zhu RQ, Gu Y (2008) The study on imidization degree of polyamic acid in solution and ordering degree of its polyimide film. J Mater Sci 43:338–344. https://doi.org/10.1007/s10853-007-1697-4

[29] Wang ZH, Chen X, Yang HX, Zhao J, Yang SY (2019) The in-plane orientation and thermal mechanical properties of the chemically imidized polyimide films. Chinese J Polym Sci 37:268–278

[30] Hao FY, Wang JH, Qi SL, Tian GF, Wu DZ (2020) Structures and properties of polyimide with different pre-imidization degrees. Chinese J Polym Sci 38:840–846

[31] Dabral M, Xia XY, Gerberich WW, Francis LF, Scriven LE (2011) Near-surface structure formation in chemically imidized polyimide films. J Polym Sci Part B: Polym Phys 39:1824–1838

[32] Fang YT, Dong J, Zhang DB, Zhao X, Zhang QH (2019) Preparation of high-performance polyimide fibers via a partial pre-imidization process. J Mater Sci 54:3619–3631. https://doi.org/10.1007/s10853-018-3068-8

[33] Chang JJ, Ge QY, Zhang MY, Liu WW, Cao L, Niu HQ, Sui G, Wu DZ (2015) Effect of pre-imidization on the structures and properties of polyimide fibers. RSC Adv 5:69555

[34] Young JA, Hinkley JA, Farmer BL (2000) Molecular simulations of the imidization of adsorbed polyamic acid. Macromolecules 33:4936–4944

[35] Nishino T, Kotera M, Inayoshi N, Miki N, Nakamae K (2000) Residual stress and microstructures of aromatic polyimide with different imidization processes. Polymer 41:6913–6918

[36] Kook HJ, Kim D (2000) In situ measurements and analysis of imidization extent, thickness, and stress during the curing of polyimide films. J Mater Sci 35:2949–2954. https://doi.org/10.1023/A:1004722609188

[37] Su JF, Chen L, Tang TT, Ren CB, Wang JJ, Qin CX, Dai LX (2011) Preparation and characterization of ternary copolyimide fibers via partly imidized method. High Perform Polym 23:273–280

[38] Park SK, Farris RJ (2001) Dry-jet wet spinning of aromatic polyamic acid fiber using chemical imidization. Polymer 42:10087–10093

[39] Kotera M, Nishino T, Nakamae K (2000) Imidization processes of aromatic polyimide by temperature modulated DSC. Polymer 41:3615–3619

[40] Kim BH, Park HJ, Park HY, Moon DC (2013) Degree of imidization for polyimide films investigated by evolved gas analysis-mass spectrometry. Thermochim Acta 551:184–190

[41] Ma XR, Zheng F, Sittert CGCE, Lu QH (2019) Role of Intrinsic factors of polyimides in glass transition temperature: an atomistic investigation. J Phys Chem B 123:8569–8579

[42] Wang XY, in 't Veld PJ, Lu Y, Freeman BD, Sanchez IC (2005) A molecular simulation study of cavity size distributions and diffusion in para and meta isomers. Polymer 46: 9155-9161

[43] Kang JW, Choi K, Jo WH, Hsu SL (1998) Structure-property relationships of polyimides: a molecular simulation approach. Polymer 39: 7079–7087.

[44] Lin DL, Li RY, Liu Y, Qi SL, Wu DZ (2021) Clarifying the effect of moisture absorption and high-temperature thermal aging on structure and properties of polyimide film at molecular dynamic level. Polymer 214:123251.

[45] Lin DL, Jiang M, Qi SL, Wu DZ (2020) Macromolecular structural evolution of polyimide chains during large-ratio uniaxial fiber orientation process revealed by molecular dynamics simulation. Chem Phys Lett 756: 137847.

[46] Lei HY, Qi SL, Wu DZ Hierarchical multiscale analysis of polyimide films by molecular dynamics simulation: Investigation of thermo-mechanical properties. Polymer 179: 121645.

[47] Lin DL, Li RY, Li TF, Xu SQ, Qi SL, Wu DZ (2021) Sol-gel transition of polyamic acid solution during chemical imidization and its effect on the drawing behavior of polyimide films. Polymer. https://doi.org/10.1016/j.polymer.2021.123842

[48] Spenley NA, Cates ME (1994) Pipe models for entangled fluids under strong shear. Macromolecules 27:3850–3858
[49] Liu XX, Qian LY, Shu T, Tong Z (2003) Rheology characterization of sol–gel transition in aqueous alginate solutions induced by calcium cations through in situ release. Polymer 44:407–412
[50] Yin CQ, Dong J, Zhang ZX, Zhang QH (2014) Rheological behaviour of polyamic acid spinning solutions containing heterocycle. Mater Res Innov 18:803–807
[51] Dikshit AK (2012) Rheological behaviours of polyimide precursor in organic solvents for coating on silica optical fibre. Polym-Plast Technol 51:707–715
[52] Zhang MY, Niu HQ, Lin ZW, Qi SL, Chang JJ, Ge QY, Wu DZ (2015) Preparation of high performance copolyimide fibers via increasing draw ratios. Macromol Mater Eng 300:1096–1107